Effects of heat on new and aged polyamide 6,6 textiles during pest eradication

CrossMark

E. Richardson [a],*, G. Martin [b], P. Wyeth [c]

[a] Department of History of Art, University College London, Gower Street, London WC1E 6BT, UK
[b] Victoria and Albert Museum, Cromwell Road, London SW7 2RL, UK
[c] Centre for Textile Conservation, University of Glasgow, Glasgow G12 8QQ, UK

A B S T R A C T

Subjecting artefacts to raised (58 °C) or lowered (−30 °C) temperatures in order to combat the problem of pest infestations is common practice within the museum and heritage sector. However, concerns have been raised by the conservation profession about applying temperature based pest treatments to polyamide 6,6, due to the changes in thermal properties known to occur over the range of temperatures in question.

Unaged and artificially aged polyamide 6,6 fibres were subjected to creep/recovery experiments using dynamic mechanical analysis at temperatures ranging from 58 °C to −30 °C. These experiments were carried out on loaded samples to determine whether textile material would suffer deterioration if treated whilst hanging under load, for example on a mannequin. Samples were analysed before and after loading by attenuated total reflectance Fourier-transform infrared spectroscopy, differential scanning calorimetry and tensile testing to investigate the chemical and physical alterations in the polyamide 6,6 fabric subject to treatment.

Samples loaded at room temperature exhibited permanent contraction, attributed to strain induced crystallization. For both the unaged and aged samples at elevated temperatures the samples underwent permanent deformation. Samples treated at sub-ambient temperatures recovered to their original length during the recovery section of the creep test, although some structural alterations were evident during subsequent analysis. The results suggest that the low temperature treatments of polyamide artefacts, particularly in the presence of stress, are preferable.

1. Introduction

In recent years there has been growing interest in synthetic materials within the heritage sector; both for identification purposes and in order to determine their physical condition [1–5]. Since their development in the late 19th Century, synthetic polymers have moved steadily into almost every area of life and, as a consequence, into a growing number of museum collections.

The application of raised and lowered temperatures to combat the problem of pest infestations are common within museum and heritage environments. Pinniger [6] states that pests need just four key things for sustainable life: food, harbourage, warmth and water (or humidity). This therefore makes all organic based museum collections vulnerable to attack by insect pests, as they supply a ready source of food. A number of studies have been carried out into the effects of heat and freezing treatments on natural cellulosic and proteinaceous materials [7–11], but their impact on synthetic materials has not been thoroughly studied in a museum collection context. This is due to the fact that synthetic polymers do not provide a source of food for insects. Nevertheless, they are widely found in conjunction with natural polymers, in composite materials, as decorative elements and fasteners, or used in conservation treatments and, as such, it becomes necessary to concurrently treat synthetic material during an infestation. For example, Nylon 6,6 netting is used as a support material during the conservation of fragile textiles, such as upholstery and wall hangings [12].

When an infestation arises there are a number of options available to conservators designed to resolve the problem. These include fumigation, anoxia, or raised and lowered temperature treatments. The latter two approaches are most commonly applied within the heritage sector, due to the relatively low cost of implementation, and the short time periods required to achieve insect mortality. When raising temperatures the majority of the stages in

* Corresponding author.
E-mail address: E.Richardson@ucl.ac.uk (E. Richardson).

insect pest life cycles, from eggs through to adult, are killed when exposed to temperatures of 52 °C, with the exception of the House Longhorn beetle, which requires temperatures of 55 °C [4,13]. The relative humidity (RH) surrounding the object is key to it maintaining dimensional stability, due to the moisture equilibrium of an object within its surrounding atmosphere [13]. This can be achieved either by enclosing small objects in sealed bags [10], or on a larger scale, via the Thermo Lignum WARMAIR® process. This latter case is a commercial process that employs a large temperature and RH controlled insulating chamber [14].

Low temperature treatments rely on the fact that most insect pests will die when exposed to a rapid drop in temperature to below −18 °C. Although there are some species which will survive temperatures down to around −40 °C, these are not problematic in the context of collection infestations [6]. The accepted protocol for low temperature eradication is to subject objects to −18 °C for 14 days or to −30 °C for a duration of 72 h [15]. Any object subject to freezing temperatures is bagged prior to treatment and as much air removed from the surrounding space as possible. These bags act as a barrier between the external air and the object surface, reducing the risk of condensation on the item as it is acclimatised after treatment. If condensation does form on the surface of a porous material then moisture may be adsorbed. This poses problems for heritage artefacts, causing dimensional changes at the surface of an object, alterations in elastic properties of material under tension, migration of colourants, and water staining.

A lack of knowledge and understanding of complex synthetic polymers proves problematic when conservators are required to treat or advise on stability. Kite [16] has suggested that being able to identify the materials susceptible to chemical or physical damage during or after treatment would enable informed decisions when faced with pest infestations. The relatively limited work carried out in the conservation sector regarding the effects of temperature treatments on organic artefacts has been primarily related to structural changes induced by the phase change of moisture between object and the surrounding atmosphere [7,9,17]. There has been limited attention given to the physical characteristics and chemical stability of the materials themselves, especially in relation to the aged and degraded states in which many museum objects are found.

In addition to the vulnerability of heritage artefacts, many of these objects have intrinsic or historical value, which means longevity is key. Therefore, any preventive or interventive conservation treatments should avoid exacerbating degradative processes. Shashoua [18] cites a case where the degradation of rubber had an adverse effect on its behaviour at low temperatures. In this case, trial low temperature storage to reduce the rate of deterioration of synthetic polymers, at the National Air and Space Museum in Washington DC, resulted in a permanent loss of flexibility in sections of a space suit. The reduction in temperature was well above that stated for loss of elasticity in new vulcanised rubber, therefore this change in property was regarded as a consequence of deterioration. This indicates that the types of material held within heritage collections do not necessarily behave in a manner to be expected in new material and highlights the need for a thorough understanding of the behaviour of aged material at various temperatures.

During consultation with a number of conservators on this matter, it became apparent that one area of particular interest was the treatment of synthetic polymers, with the stability of polyamide 6,6 being raised as one of primary concern [19–22]. Such concerns stem from the changes in thermal properties known to occur over the range of temperatures used for thermal pest treatments. Polyamides are long chain synthetic molecules formed through step polymerisation mechanisms and are characterised by the presence of the amide functional group linking one or more

type of monomer unit [23]. Quoted values for the glass transition temperature (Tg) of aliphatic polyamides tend to place the transition in the region of 42–55 °C, depending on the subclass [24]. Therefore, when raising temperature levels during pest control treatments unaged aliphatic polyamides will pass through their Tg; this transition having implications for the physical strength of a material. At temperatures above the Tg the molecules increasingly move freely, and deform readily to external forces giving permanent deformation by a combination of elastic and viscous flow. Lowering a material to well below its Tg will produce a substance resistant to loading, which is stiff and rigid in nature. It is therefore possible that museum objects containing these classes of polymer may become vulnerable to physical changes during treatments that prove detrimental to their short and long term stability.

In the work presented here polyamide 6,6 woven yarns were subjected to temperature pest control treatments with a view to determining the physical stability of such material when treated in conjunction with natural fibres.

It is well documented that polyamide fibres and nets suffer significant degradation in the presence of UV, causing the material to yellow and become brittle [25–27]. Photooxidative reactions are free radical reactions and have been reported to continue after the incident radiation has been removed, caused by residual free radicals remaining in the polymer structure [28]. This last point raises the question about the stability of aged polyamide in elevated temperature treatments. Working above the Tg removes restrictions on molecular motion, potentially allowing radicals to move freely throughout the polymer structure, thus accelerating degradation. In the current work samples were subjected to photodegradation prior to treatment to determine the impact of age on stability.

2. Materials and methods

2.1. Materials

The test material used throughout the work presented here was a polyamide 6,6 ISO Single Adjacent Fabric made in accordance with ISO Section F03 [29]. The polyamide 6,6 fabric was used (as received) before and after subjecting it to photodegradation. The fabric was an undyed, plain-weave structure, with 20 warps and 20 wefts per cm², weighing 125 g/m². The warps were double Z-plied yarns and the wefts single yarns. A double Z-plied yarn refers to an assembly of two previously twisted yarns, with a right hand twist. The twist is determined by looking down the length of the yarn, and the progression of the twist away from the observer describing the direction. The two types of yarn twists are Z and S, referring to the central diagonal sections of each letter. Supplied by Testfabrics Inc., the fabric was received washed and scoured in an alkaline bath to remove processing oils and starches. Yarn fabric was studied in place of single fibre testing as this most closely represented the type of material found in heritage collections.

Table 1 contains a summary of results for each of the samples studies, before and after treatment.

2.2. Accelerated degradation

The nature of museum and heritage objects often precludes their use for analysis and testing. It therefore becomes necessary to artificially age model material, using conditions that can be tentatively related to the environmental history of an object. Light, heat and humidity are the common factors that promote natural ageing in polymers [30].

A set of samples were exposed to artificial sunlight using a Q-Sun Xenon test chamber Xe-1 fitted with a Xenon arc lamp. A daylight filter was fitted between the source and the samples and

Table 1
Summary of experimental conditions for each sample and their corresponding tensile properties, polarized ATR D values, percentage crystallinity, thermal transitions and creep/recovery strain.

Sample	Treatment	Breaking load/N	Strain/%	Ratio 0/90 D_{1196}	Ratio 0/90 D_{1416}	Ratio 0/90 D_{1691}	Crystallinity/%	T_m/°c	T_g/°c	Initial Strain/%	Final loaded strain/%	Final strain after recovery/%
Con Aa	Unaged	286.7±7.8	34.6±0.7	1.89±0.06	0.34±0.01	0.38±0.03	54.7±0.8	266.8±0.3	35.3±0.8			
Con A 23	Unaged, Creep at 0.3 MPa, 23 °C			1.87±0.32	0.33±0.06	0.39±0.07	57.2±1.0	264.2±0.2	35.7±0.6	0.56	0.48	−0.11
Con A 58	Unaged, Creep at 0.3 MPa, 58 °C			1.58±0.17	0.45±0.07	0.54±0.05	53.2±0.8	265±0.2	32.3±0.4	0.82	1.2	0.45
Con A −30	Unaged, Creep at 0.3 MPa, −30 °C			1.49±0.03	0.45±0.02	0.55±0.02	52.4±0.8	267±0.2	36.1±1.0	0.41	0.49	0.02
Con Bb	UV Aged	114.1±3.8	19.5±0.6	1.94±0.03	0.30±0.02	0.33±0.02	51.9±0.2	263.2±0.2	33.2±0.6			
Con B 23	UV Aged, Creep at 0.3 MPa, 23 °C			1.49±0.08	0.46±0.08	0.43±0.09	56.3±0.4	265±0.2	31.6±0.5	0.45	0.07	−0.32
Con B 58	UV Aged, Creep at 0.3 MPa, 58 °C			1.76±0.14	0.32±0.05	0.41±0.04	55.3±0.7	264.1±0.2	33.0±1.0	0.89	1.05	0.37
Con B -30	UV Aged, Creep at 0.3 MPa, −30 °C			1.85±0.02	0.35±0.01	0.45±0.01	53.2±0.9	263±0.9	31.3±0.6	0.64	0.80	0.00

irradiance was set at 0.68 W/m^2 (340 nm). This produced a spectral power distribution equivalent to summer sunlight, with a total dose of 40 MJ/m^2 over one day. The samples were aged for 168 h, equating to approximately 20 days of exposure. Samples were aged under extreme conditions as the majority of textile artefacts have been exposed to natural daylight previous to acquisition. The position of the samples in the ageing chamber were exchanged with each other daily to ensure even exposure, preventing differential ageing.

2.3. Dynamic mechanical analysis

Dynamic Mechanical Analysis (DMA) was employed to monitor the creep and creep recovery behaviour of the samples at isothermal temperatures with a static load simulating beaded garments. It was calculated that the force experienced on the upper fibres of a typically heavily beaded garment was of the order of 0.5 N, giving a stress on the specimen fibres of approximately 0.3 MPa. The decision was taken to study woven fabric under load after consultation with textile conservators [20,21], who suggested that it would be of benefit to understand the impact of treating mounted garments. If found to be safe, the ability to carry out such treatments, without the need for removal from mannequins, would save time during preparation. The results relating to samples treated without the presence of a load have been published elsewhere [33].

Creep/recovery analyses were carried out using TA Instruments DMA Q800 analyser fitted with a film tension clamp and purged with compressed air. Samples were 10 warp yarns wide measuring approximately 5 mm, with a gauge length of 16 mm and a preload of 0.001 N. The initial gauge length varied when the lower section of the sample was clamped into place. Once the clamp was in place the instrument determines the actual gauge length with the software subsequently accounting for this during the calculation of the percentage strain. The sample cell was then taken to the temperature of interest and allowed to equilibrate for 5 min before the programmed stress was applied. The samples remained subject to the applied load for 150 min and were then allowed to recover for 300 min on removal of the load. Isothermal conditions were maintained throughout the experiment. Relative humidity levels were not controlled during testing and it should be borne in mind that the presence of moisture may induce plasticization of the polymer chains.

2.4. Tensile analysis

Tensile tests were carried out to monitor the mechanical strength of the woven fabric before and after photodegradation, in order to better understand the material under study. Mechanical testing was performed in tension using an Instron 5544 Materials Tester fitted with a 1 kN load cell. Tensile testing was carried out following a modified strip test method, BS EN ISO 13934-1:1999 [31], with a gauge length of 80 mm, extension rate of 10 mm/min, and sample width of 20 warp yarns wide, corresponding to approximately 10 mm in width. Tensile data presented relate to the average of seven repeat tensile tests. Temperature and relative humidity fluctuations averaged 21 °C ± 1 and 50% ± 4, respectively.

2.5. Fourier-transform infrared spectroscopy

Infrared analysis was carried out using a Perkin Elmer Spectrum One Fourier transform infrared (FTIR) spectrometer, fitted with a Universal attenuated total reflectance (ATR) accessory with a diamond/zinc selenide crystal. A scan range of 4000–700 cm^{-1} was employed, with a wavenumber resolution of 4 cm^{-1} and scan accumulation of 32. Polarized ATR (Pol ATR) experiments were

employed to monitor alterations in the anisotropy (directionality). A polarizer set to 0° was placed between the source and the ATR crystal and the fibre sample was rotated between 0 and 90° [32]. Dichroic peaks were identified at 1196 cm^{-1} (parallel), 1416 cm^{-1} (perpendicular) and 1631 cm^{-1} (perpendicular). The polarized ATR D values contained in Table 1 relate to the dichroic ratios calculated after normalising against non-dichroic bands as an internal reference, presented as the average of three replicates. For a detailed discussion of the methodology the reader is referred elsewhere [33].

2.6. Differential scanning calorimetry

Differential scanning calorimetry (DSC) was employed to monitor alterations in the crystalline structure before and after treatment. DSC analysis was carried out using a Perkin Elmer Power Compensated Pyris 1 DSC controlled instrument using Pyris software and coupled with a Perkin Elmer CCA7 temperature controller. The cell and furnace were purged with nitrogen at a flow rate of 30 ml/min, and the samples heated from −35 °C to 300 °C at a rate of 20 °C per minute. Liquid nitrogen was used to reduce the sample cell to sub-zero temperatures. The fabric samples were prepared in rectangular pieces measuring 7 × 7 yarns each, in order to reduce the amount of variability in contact with the sample and crucible, causing inhomogeneous heat transfer. The copper crucible was accurately weighed with and without the sample, with samples averaging an approximate mass of 2 mg.

Heating curves provide information on the crystallinity of the samples. Assuming a two-phase morphology, the percent crystallinity can be determined from the heat of melting:

$$\% \text{ Crystallinity} = \left[\Delta Hm / \Delta Hm^{\circ}\right] \times 100 \qquad (1)$$

where ΔHm° is the heat of melting of a 100% crystalline reference of the same material, and ΔHm (in J/g) refers to the sample of interest. The literature values for the heat of fusion of a 100% crystalline polyamide 6,6 range from between 191 J/g [34] to 255 J/g [25]; this

latter value being particularly high. For the work presented here the value was taken as 196 J/g, as is quoted in the Polymer Handbook by Brandrup et al. [35] and others [36,37]. ΔHm was determined by integration of the area under the temperature of melt (Tm) curve.

The Tg, being a secondary transition, does not occur at a single point, but over a temperature range. In the work presented here, Tg values refer to the mid-point of the transition i.e. the temperature at which one half of the change in the heat capacity has occurred (ΔCp). This was determined by calculating the second derivative of the heating curves. Quoted values are the average of three repeat tests.

3. Results and discussion

Table 1 contains the tensile data, and polarized ATR D values, along with the DSC and DMA-derived crystallinities, melting temperatures (Tm) and glass transition (Tg) temperatures.

A comparison of the data for the control samples A and B suggests that photodegradation, which will encourage polymer chain disruption, compromises mechanical performance significantly. Photodegradation also results in somewhat reduced crystallinity of the bulk fibre and a lowering of Tm and Tg, although the surface crystallinity, as reflected in the ATR D values remains much the same. The alteration in crystallinity is very small when sample variations are accounted for, but is contrary to what may be expected during photodegradation.

3.1. Creep/recovery experiments for control samples at room temperature

The creep/recovery curves for ambient temperature show a surprising though similar behaviour for the unaged and aged materials, Aa and Ba respectively (Fig. 1). The application of a small static load (0.3 MPa) causes an initial instantaneous elongation, due to the extension of the woven yarns in combination with elastic deformation. There is then progressive contraction of the samples,
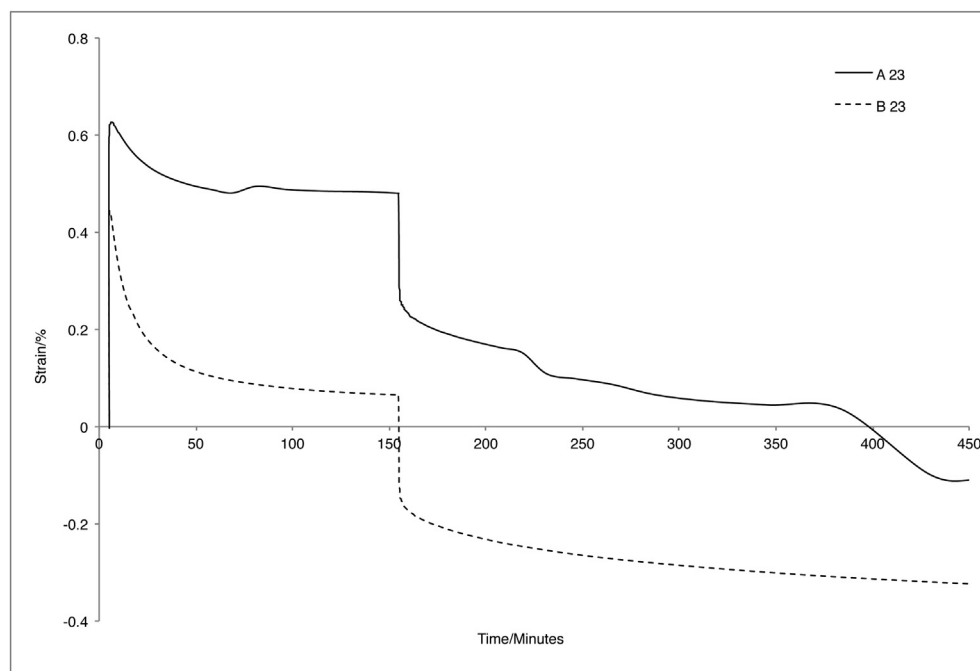

Fig. 1. DMA creep/recovery curves for samples A 23 (solid) and B 23 (dashed) at room temperature and stressed with 0.3 MPa.

somewhat more exaggerated in the aged material, and evidence of permanent strain induced crystallisation in both. Detailed analysis confirms that loading at room temperature (Table 1) effects increased bulk crystallinity, with the alignment induced during filament production by drawing of a polymer under a uniaxial load. In contrast, there is strain induced surface disordering of the aged fibres (the ATR D values approach 1). UV-promoted chain scission will increase the number of reaction sites available for cross-linking, particularly towards the outside of the fibres, resulting in a relatively brittle surface, and consequent facile chain rupture and crystallite disorientation.

After 150 min the static load was removed and the sample allowed to recover; after the load is removed the strain is instantaneously reduced due to relaxing of the woven yarns. This is followed by further gradual contraction of the samples. At the end of the experiment (450 min) both samples are shorter than their initial length. It should be noted that the instantaneous recovery strain is much less than the initial loading elastic strain.

The initial extension and drawing of the polymer chains causes an alignment of the amorphous regions in the bulk. This in turn would bring the amide groups into close proximity to each other, enabling inter-chain bonding. Murthy et al. [38] showed that there is a density increase, alongside increased crystallinity, on the cold drawing of polyamide 6 fibres. The new, ordered crystal structures occupy a reduced space, which may be seen as a contraction in the sample. If the density of the crystalline phase is taken to be 1.24 g/cm^3, and the amorphous phase 1.09 g/cm^3 [39], a simple calculation [Appendix 1] shows that the percentage change in crystallinity calculated from the DMA data gives a volume change that would account for the contraction observed. It is therefore proposed that strain induced crystallisation is occurring in the creep/recovery experiments at room temperature, for both unaged and UV-aged samples.

It is worth noting that in these experiments it is the creep under load that is of primary interest. The final creep strains before the load is removed, 0.48% (Aa) and 0.07% (Ba), represent the displacements that would be seen in the woven yarns of unaged and aged beaded dresses hanging under their own weight at ambient temperatures. These can be taken as the baselines for comparison with those samples treated at raised and lowered temperatures for pest eradication simulation.

3.2. Creep/recovery experiments for unaged samples at raised and lowered temperatures

The gradual contraction under load exhibited at 23 °C, after the initial, rapid displacement, is not seen at 58 °C. For A58 the strain continues to increase, but at a slower rate (Fig. 2). This is attributed to the extension and rearrangement of the amorphous polymer chains subjected to load above the glass transition temperature. This discontinuity occurring at 17 min may be caused by a slippage movement in the crystal structure of the polymer, similar to that proposed by Zaukelies [40] for polyamide 6,6 crystallites in bristles. At 58 °C the final strain under load is double that seen at room temperature, while after relaxation, at the end of the creep test, the sample held above Tg (A58) is 0.7% longer than that at ambient (A23). This suggests that raised temperature treatments of a hanging garment may have a noticeable effect on the fabrics dimensions.

For the sub-ambient sample A-30, the initial displacement is reduced to 0.41% (compared to 0.56% for A23), due to a somewhat more rigid structure (Fig. 2). The low temperature decreases chain mobility, possibly with the additional constraint of the freezing of sorbed moisture. There is no strain induced contraction, with the reduced mobility in the polymer chains preventing rearrangement to new conformations and inhibiting crystallization. On removal of the load the sample returns to its original length in a typical viscoelastic manner.

The further ATR and DMA-derived results (Table 1) suggest reduced crystallinity of the bulk and increased anisotropy at the fibre surface following both high and low temperature regimes. Strain induced crystallisation is inhibited in both cases.

For the unaged material, the final displacement under load was significantly higher at 58 °C than at room temperature. Although it
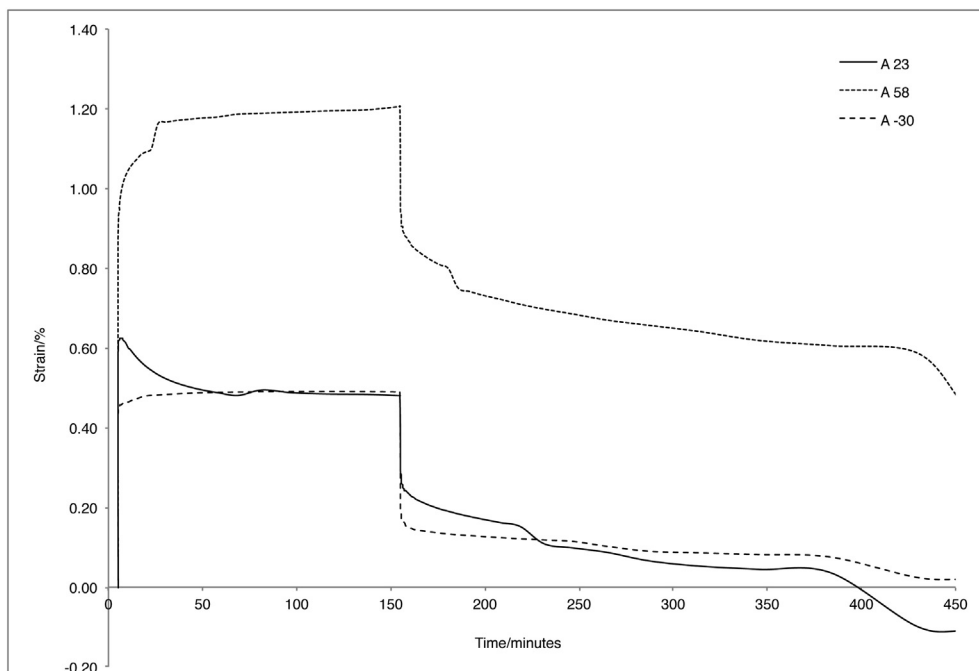

Fig. 2. DMA creep/recovery curves for samples A 23 (solid), A 58 (dotted) and A -30 (dashed) and stressed with 0.3 MPa.
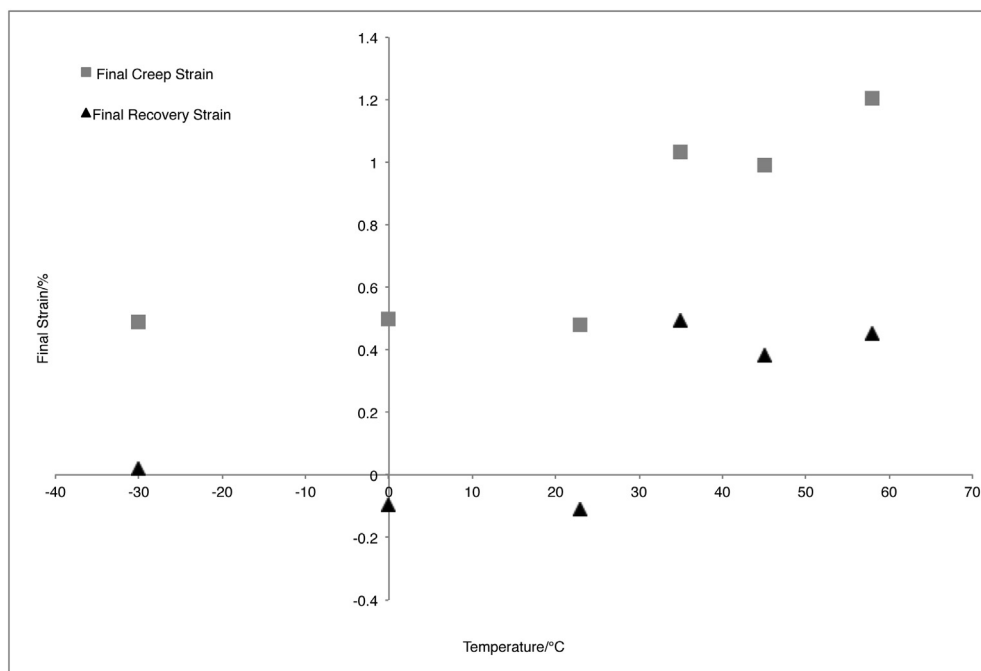
Fig. 3. Final creep strain (grey) and final recovery strain (black) versus temperature for all unaged samples (A) at six different temperatures and stressed with 0.3 MPa.

is the creep section that is of primary interest, the fact that the sample did not fully recover after 450 min indicates permanent deformation, associated with underlying structural changes. At −30 °C, the sample displacement at the end of the creep section was found to be equal to that at 23 °C. This, coupled with the fact that the sample A-30 recovered fully, indicates that the low temperature treatment of unaged polyamide would be the preferred method for pest eradication.

To further elucidate these differing behaviours, supplementary experiments were carried out at intermediate temperatures of 0, 35 and 45 °C. The final creep strains under load at 150 min, and the permanent deformation strains at the end of the relaxation period are plotted for all the unaged samples in Fig. 3. The trends are consistent with increased displacements above ambient, as the temperature moves through the glass transition (around 35 °C). The general trend below room temperature is one of restricted deformation.
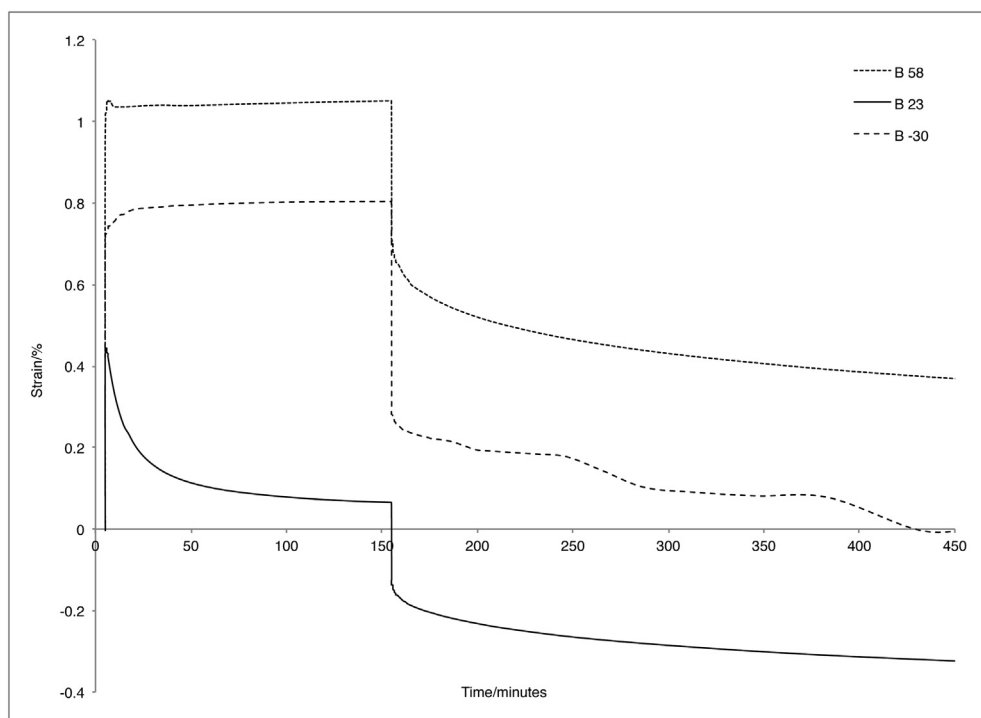

Fig. 4. DMA creep/recovery curves for samples B 23 (solid), B 58 (dotted) and B −30 (dashed) and stressed with 0.3 MPa.

3.3. Creep/recovery experiments for aged samples at raised and lowered temperatures

While the slow deformation phase under load is not observed for the aged specimen, at 58 °C a broadly similar DMA creep/recovery pattern emerges for the aged sample, B58, as for the unaged sample, A58 (Figs. 2 and 4). Furthermore, the various DSC and DMA derived parameters are comparable for these two specimens (Table 1). For B58 the initial displacement is slightly lower than for the unaged sample, as may be expected for a cross-linked specimen; the latter may also account for the absence of the slowly increasing strain phase.

In contrast, at low temperature the aged sample, B-30, produces quite distinct thermal and mechanical parameters (Table 1). The initial displacement is considerably higher than that seen at ambient temperature (Fig. 4), and much of this is recovered immediately on load removal. This is unexpected given the reduction in temperature and reduced molecular mobility, but is possibly due to enhanced moisture penetration into the yarns as a consequence of fluctuations in relative humidity.

As with the unaged material, A-30, the strain-induced contraction seen at room temperature, following the initial rapid displacement, does not occur. At low temperatures rearrangement of the polymer chains is too slow, and crystallisation is prevented on the experimental timescale [41]. In the recovery section of the curve, it can be seen that after removal of the stress sample B-30 returns to its original length, in the same way as the unaged sample A-30.

The final displacement under load, and final strain after recovery (Table 1), for samples B-30 and B58 indicate that sample deformation is significantly reduced at lowered compared to elevated temperatures. This general pattern is also noted for the unaged specimens.

The final displacement under load, and final strain after recovery, indicate that sample deformation is reduced at lowered temperature than at elevated temperatures. However, there are clearly effects that are bigger than those seen at room temperature for a loaded sample, and this may suggest that treatment of textile artefacts, both new and aged, should not be carried out whilst they are hanging under their own weight. When textiles are to be subject to these pest control treatments, where possible, they should be removed from their mannequins or frames and laid horizontal to minimise stress.

The results of this study may have broader implications in relation to low temperature storage for the retardation of degrading polymers. Exposing new polyamide 6,6 yarns to temperatures below ambient was not shown to induce any permanent deformation under load; the trend being one of restricted deformation, which illustrates the need for careful handling to avoid brittle damage. For aged material below room temperature the dimensional alterations clearly suggest the need for horizontal storage, as previously concluded for the treatment of polyamide 6,6 during pest eradication.

4. Conclusions

The unaged polyamide 6,6 woven yarns were shown to be moderately crystalline with a well oriented outer layer. Photodegradation led to reduced mechanical performance, attributable to scission along the polymer chain and some cross-linking. These two control materials were subsequently exposed to environments simulating pest control treatments, where the samples were subjected to creep/recovery loading using a DMA apparatus.

For the unaged material, the creep/recovery curves exhibited interesting patterns of behaviour. At elevated temperatures, the strain induced crystallisation that had been apparent at room temperature was prevented, due to increased chain mobility. Rather, it was found that, after the initial displacement, there was a slow increase in strain associated with the extension of the amorphous regions. This was followed by a sudden displacement, before reaching a constant creep rate. This discontinuity was assigned to a tilting and slippage in the crystalline regions. There was incomplete recovery of deformation at elevated temperature. At sub-ambient temperatures, creep of the unaged material was hindered by mobility restrictions. This resulted in reduced initial displacement and an absence of strain induced crystallisation. The final recovery strain indicated that unaged, loaded polyamide at −30 °C did not suffer any permanent deformation.

The aged material presented somewhat different behaviour from that exhibited by the unaged samples. With all other parameters being equal, these differences were attributed to the structure of the starting material. At an elevated temperature the sample showed a somewhat reduced initial displacement, consistent with some chain cross-linking, and it did not exhibit the strain induced contraction seen at room temperature. At low temperature there was an unexpectedly high initial displacement, larger than that seen at room temperature, possibly due to sorbed moisture. The same creep behaviour was observed as for the unaged sample; initial displacement settling to an almost constant strain rate, the reduced energy preventing strain induced contraction. On removal of the load, there was complete recovery.

In relation to the loaded textiles, the analyses clearly shows a greater degree of strain and irreversible creep behaviour at raised temperature, for both unaged and aged samples. In contrast, the samples proved relatively stable at sub-ambient temperatures. Although the experimental parameters may not exactly match those of the pest control methods, they serve as an indication of how the unaged and aged material may behave under such treatments. Thus low temperature treatments of polyamide textile artefacts should be preferred, particularly in the presence of stress caused by adornments, and arrangement on mannequins or frames.

Appendix 1. Calculation of volume change caused by increased crystallinity

The mass of a fibre is equal to volume multiplied by density (V_1P_1), with the volume being equal to $\pi r^2 L$. On contraction, the mass remains constant, therefore:

$$V_1P_1 = V_2P_2$$

$$P_1 \times \pi r_1^2 L_1 = P_2 \times \pi r_2^2 L_2$$

where:

V_1 is the initial volume of the fibre
V_2 is the final volume of the fibre
P_1 is the density of the amorphous phase = 1.09 g/cm^3
P_2 is the density of the crystalline phase = 1.24 g/cm^3

L_1 the initial fibre length = 80 mm
L_2 the final fibre length
r^2 is the diameter of the fibre

Assuming a two-phase model, as the density increases with increasing crystallinity, the volume will decrease:

$$P_1 \times \pi r_1^2 L_1 / P_2 = \pi r_2^2 L_2$$

If we assume that the radius of the fibre remains constant:

$$L_1 P_1 / P_2 = L_2$$

$$1.09 \times 80 / 1.24 = 70.3 \text{ mm}$$

Full crystallization would lead to a reduction in length of 9.7 mm.

On application of a 0.3 MPa load at room temperature the samples exhibited an increase in crystallinity of 2.5% for Con A 23 and 4.4% for Con B 23 (Table 1), giving a calculated contraction in the length of the samples:

Sample A 23 $-9.7 \times 2.5 / 100 = -0.24 \text{ mm} = -0.3\%$ strain

Sample B 23 $-9.7 \times 4.4 / 100 = -0.43 \text{ mm} = -0.55\%$ strain

It should be born in mind that these values assume that the radius of the fibres remain constant and that the matrix follows a two-phase model.

References

[1] Lavedrine B, Fournier A, Martin G, editors. POPART: preservation of plastic artefact in museum collections. Paris, France: Le Comité des Travaux Historiques et Scientifiques; 2012.
[2] Waentig F. Plastics in art. Petersburg: Michael Imhof Verlag; 2009.
[3] Keneghan B, Egan L, editors. Plastics: look at the future and learning from the past. London: Archetype Publications in association with the Victoria and Albert Museum; 2007.
[4] Rogerson C, Garside P, editors. The future of the 20th century: collecting, interpreting and conserving modern materials. London: Archetype Publications; 2005.
[5] Corzo MA, editor. Mortality immortality? The legacy of 20th century art. Los Angeles: J.Paul Getty Trust; 1998.
[6] Pinniger D. Pest management in museums, archives and historic houses. London: Archetype Publications; 2001.
[7] Beiner GG, Ogilvie TM. Thermal methods of pest eradication: their effect on museum objects, vol. 29. The Conservator; 2005/06. pp. 5–18.
[8] Berkouwer M. Freezing to eradicate insect pests in textiles at Brodsworth, vol. 18. The Conservator; 1994. pp. 15–22.
[9] Ackery PR, Testa JM, Ready PD, Doyle AM, Pinniger DB. Effects of high temperature pest eradication on DNA in entomological collections. Stud Conservat 2004;49:35–40.
[10] Xavier-Rowe A, Imison D, Knight B, Pinniger D. Using heat to kill museum insect pests: is it practical and safe?. In: Proceedings IIC advances in conservation: contributions to the melbourne congress 2000. pp. 206–11.
[11] Carrlee E. Does low-temperature pest management cause damage? Literature review and observational study of ethnographic artefacts. J Am Soc Conserv 2003;42:141–66.
[12] Sinha MK, Christie RM, Shamey R. The effect if acid dyes on the photo-degradation of knitted Nylon conservation support net. In: Postprints of the future of the 20th century: collecting, interpreting and conserving modern materials. London: Archetype Publications; 2005. pp. 92–9.
[13] Strang TJK, Dawson JE. Technical bulletin no 12: controlling museum fungal problems. Ottawa: Canadian Conservation Institute; 1991.
[14] Child B. The Thermo Lignum process for insect pest control. Paper Conservation News 1994;72:9.
[15] Wellheiser JG. Nonchemical treatment process for disinfestation of insect and fungi in library collections. Munich: K.G. Saur; 1991.
[16] Kite M. Head of furniture, textiles and frames section. London: Victoria and Albert Museum; 10 August 2006 [Personal Communication].
[17] Ackery PR, Doyle A, Pinniger D. Safe high temperature pest eradication − is the answer in the bag? Biol Curator 2002;22:13–4.
[18] Shashoua YR. Freezing the present to preserve the future. In: The future of the 20th century−collecting, interpreting and conserving modern materials. London: Archetype Publishers; 2005.
[19] Quye A. Principal scientist. Edinburgh: National Museums of Scotland; 6 December 2006 [Personal Communication].
[20] Haldane EA. Textile conservator, furniture, textiles and frames section. London: Victoria and Albert Museum; 17 January 2008 [Personal Communication].
[21] Howard S. Textile conservator. Hampshire County Council Museum and Archives Service; 19 March 2007 [Personal Communication].
[22] Foskett S. Textile conservator. National Museums of Scotland; 15 February 2007 [Personal Communication].
[23] Brydson J. Plastics materials. Oxford: Butterworth-Heinemann; 1999.
[24] Gordon GA. Glass transitions in nylons. J Polym Sci Part A-2 1971;9:1693–702.
[25] Sinha MK. An investigation of photodegradation of a support netting used in the conservation of historic textiles. Edinburgh: Heriott-Watt; 2006.
[26] Do CH, Pearce EM, Bulkin BJ, Reimschessel HK. FT-IR spectroscopic study on the photo- and photooxidative degradation of nylon. J Polym Sci Part A Polym Chem 1987;25:2301–21.
[27] Egerton GS. Some aspects of the photochemical degradation of nylon, silk and viscose rayon. Textil Res J 1948; November:659–69.
[28] Allen NS, Edge M, Horie CV. Polymers in conservation. Cambridge: Royal Society of Chemistry; 1992.
[29] British Standards Institution. Textiles−tests for colour fastness. BS ISO 105: Part F03; 2001 [London].
[30] Erhardt D, Mecklenburg MF. In: Proceedings materials Research Society Symposium 1995.
[31] British Standards Institution. Textiles−standard atmospheres for conditioning and testing. BS EN 20139:1992 ISO 139; 1973 [London].
[32] Bolterauer C, Helmut H. Calculation of IR dichroic values and order parameters from molecular dynamics simulations and their application to structure determination of lipid bilayer. Eur Biophys J 1996;24:322–33.
[33] Richardson E. Investigating the characterisation and stability of polyamide 6,6 in heritage artefacts. Textile Conservation Centre. Southampton: University of Southampton; 2009.
[34] Simal AL, Martin AR. Structure of heat-treated nylon 6 and 6.6 fibres I: the shrinkage mechanism. J Appl Polym Sci 1998;68:441–52.
[35] Brandrup J, Immergut EH, Grulke EA. Polymer handbook. New York: Wiley; 1999.
[36] Mark JE, editor. Polymer data handbook. Oxford: Oxford University Press; 1999.
[37] Starkweather HW, Zoller P, Jones GA. The heat of fusion of 66 Nylon. J Polym Sci Part B Polym Phys 1984;22:1615–21.
[38] Murthy NS, Bray RG, Correale ST, Moore RAF. Drawing and annealing of nylon 6 fibres: studies of crystal growth, orientation of amorphous and crystalline domains and their influence on properties. Polymer 1995;36(20):3863–73.
[39] Vasanthan N, Ruetsch SB, Salem DR. Structure development of polyamide-66 fibres during drawing and their microstructure characterization. J Polym Sci Part B Polym Phys 2002;40:1940–8.
[40] Zaukelies DA. Observation of slip in Nylon 66 and 610 and its interpretation in terms of a new model. J Appl Phys 1962;33(9):2797–803.
[41] Echalier B, Bluet P, Lefebvre F. The ductile/brittle transition in polyamide 11 at low temperature. In: Polymers at low temperatures. London: Polymer Properties Group, Institute of Marine Engineers; 1987.